BMC Zoology

RESEARCH ARTICLE Open Access

Ecology and trophic role of *Oncholaimus dyvae* sp. nov. (Nematoda: Oncholaimidae) from the lucky strike hydrothermal vent field (Mid-Atlantic Ridge)

Daniela Zeppilli[1*], Laure Bellec[1,2,3,4], Marie-Anne Cambon-Bonavita[2,3,4], Wilfrida Decraemer[5], Diego Fontaneto[6], Sandra Fuchs[1], Nicolas Gayet[1], Perrine Mandon[1,7], Loïc N. Michel[1], Marie Portail[1], Nic Smol[5], Martin V. Sørensen[8], Ann Vanreusel[9] and Jozée Sarrazin[1]

Abstract

Background: Nematodes are an important component of deep-sea hydrothermal vent communities, but only few nematode species are able to cope to the harsh conditions of the most active vent sites. The genus *Oncholaimus* is known to tolerate extreme geothermal conditions and high sulphide concentrations in shallow water hydrothermal vents, but it was only occasionally reported in deep-sea vents. In this study, we performed morphological, genetic and ecological investigations (including feeding strategies) on an abundant species of *Oncholaimus* recently discovered at Lucky strike vent field on the Mid-Atlantic Ridge at 1700 m water depth.

Results: We described this species as *Oncholaimus dyvae* sp. nov.. This new species differs from all other members of the genus by the combination of the following characters: body length (up to 9 mm), the presence of a long spicule (79 μm) with a distally pointed end, a complex pericloacal setal ornamentation with one precloacal papilla surrounded by short spines, and a body cuticule with very fine striation shortly posterior to the amphid opening. Overall, *O. dyvae* sp. nov. abundance increased with increasing temperature and vent emissions. Carbon isotopic ratios suggest that this species could consume both thiotroph and methanotrophic producers. Furthermore sulfur-oxidizing bacteria related to Epsilonproteobacteria and Gammaproteobacteria were detected in the cuticle, in the digestive cavity and in the intestine of *O. dyvae* sp. nov. suggesting a potential symbiotic association.

Conclusions: This study improves our understanding of vent biology and ecology, revealing a new nematode species able to adapt and be very abundant in active vent areas due to their association with chemosynthetic micro-organisms. Faced by the rapid increase of anthropogenic pressure to access mineral resources in the deep sea, hydrothermal vents are particularly susceptible to be impacted by exploitation of seafloor massive sulfide deposits. It is necessary to document and understand vent species able to flourish in these peculiar ecosystems.

Keywords: *Oncholaimus dyvae* sp. nov., Hydrothermal vents, Deep sea, Carbon and nitrogen isotopic ratios

* Correspondence: Daniela.Zeppilli@ifremer.fr
[1]IFREMER Centre Brest REM/EEP/LEP, ZI de la pointe du diable, CS10070, 29280 Plouzané, France
Full list of author information is available at the end of the article

Background

Deep-sea hydrothermal vents are unique and severe environments. Hydrothermal fluids are formed by cold sea water which infiltrates oceanic crust. These fluids are heated and enriched with reduced chemicals sorting at very high temperatures (> 400 °C, [1]). Vent ecosystems are formed by organisms able to cope with these extreme conditions (high concentrations of reduced compounds, heavy metals and radionuclides, low oxygen level, and elevated temperatures [2, 3]). Nevertheless the severity of this environment, vents are particularly richer (in term of biomass and productivity) than the adjacent deep-seafloor [4]. This elevated macro-megafaunal density results from the obligate exploitation of a localized food source that is produced primarily by microbial chemolithoautotrophy, which in turn is directly dependent on reducing substances from vent fluids [5, 6]. Hydrothermal vent fauna interacts directly with microorganisms either through symbiosis, which provides nutrition for the most dominant large invertebrate species (e.g., siboglinid tube worms, bathymodiolin mussels, vesicomyid clams, shrimps [7]), through direct grazing on the microbial communities [6], or, in the case of species like the crab *Xenograpsus testudinatus* [8], indirectly, as they feed on microbial grazers.

Nematodes are an important component of hydrothermal vent communities worldwide in term of abundance and biomass [9–11]. Hydrothermal vent nematode communities are usually composed by a dozen of nematode taxa and dominated by two or three of them [4, 9, 10, 12–16]. Mussel bed fields of the Lucky Strike vent field (Mid-Atlantic Ridge) are usually dominated by two nematode genera: *Cephalochaetosoma* and *Halomonhystera* [9]. The genus *Oncholaimus* (only occasionally found in deep-sea vents [13]) was recently reported in deep-sea Atlantic hydrothermal vents [10, 17]. Both studies showed that *Oncholaimus* can be very abundant, reaching remarkable biomass values for the total nematode community due to its big size [10].

Nevertheless *Oncholaimus* is an important component of vent communities, information about diversity, trophy and ecological role of this group is almost unknown. In this study, we performed morphological and genetic investigations on this abundant species of *Oncholaimus* reported at Lucky strike vent field on the Mid-Atlantic Ridge at 1700 m water depth (Fig. 1), describing it as a new species for science. We also analyzed its abundance, biomass and diet and we explored its ecological role in the Lucky Strike hydrothermal vent field.

Results

Description of Oncholaimus dyvae sp. nov

Systematic

Order Enoplida Family Oncholaimidae Filipjev, 1918

Genus Oncholaimus *Dujardin*, 1845

Diagnosis of the genus based on Smol et al. [18]. Oncholaiminae. Left ventrosublateral tooth largest. Females monodelphic-prodelphic with antidromously reflexed ovary. Demanian system well developed, terminal ducts and pores present in variable number or absent in virgin females. Males diorchic. Spicules short, gubernaculum absent. Tail short

Oncholaimus dyvae sp. nov

Material

Male holotype 14 paratype males and 11 paratype females

Type material is deposited in the Natural History Museum of Denmark (holotype NHMD-115822, paratypes from NHMD-115823 to NHMD-115832). This species is deposited in ZooBank with accession number urn:lsid: zoobank.org:pub:38105B1C-9E7D-42FD-BF74-D403218D12A5.

Measurement

See Table 3.

Etymology

This species is named in honour of the project DYVA (Deep-sea hYdrothermal Vent nematodes as potential source of new Antibiotics) that supported this study.

Males

Body length 9430 μm, maximum diameter 95 μm, with a smooth cuticle (Fig. 2a, Table 1). Habitus very long and slender, slightly anteriorly tapered, but more pronounced in tail region; body cuticle smooth in light microscopy but showing fine striation shortly posterior to the amphid opening (see Fig. 3c and Fig. 4f).

Six conical lips deeply separated, each bearing 1 minute rounded inner labial papilla (Fig. 3a,b,c,d). Ten setae (six outer labial and four cephalic) in one circle (Fig. 3a, b) both equally 11 μm long. Head diameter 40 μm. Ample buccal cavity characterized by sclerotized walls. Three unequal teeth (onchs): two small teeth (dorsal and right ventrosublateral) and one large left ventrosublateral tooth. Onchs with ventral subapical outlets of the oesophageal glands, one dorsal and two ventrosublateral pharyngeal glands (Fig. 3a). Amphideal fovea wide cup-shaped with elliptical opening 0.3 of the corresponding body diameter, located at 15 μm from anterior end. Amphid fovea is 18 μm in width (0.4 c.b.d.) and 9 μm in height (Fig. 3c.d.e).

Somatic setae (9 μm long) arranged in six longitudinal rows (Fig. 3f). Oesophagus muscular and cylindrical (810 μm length, 1/10 times body length). Secretory-excretory pore opening at 172 μm from anterior end (at about 0.2 times oesophagus length from anterior end;

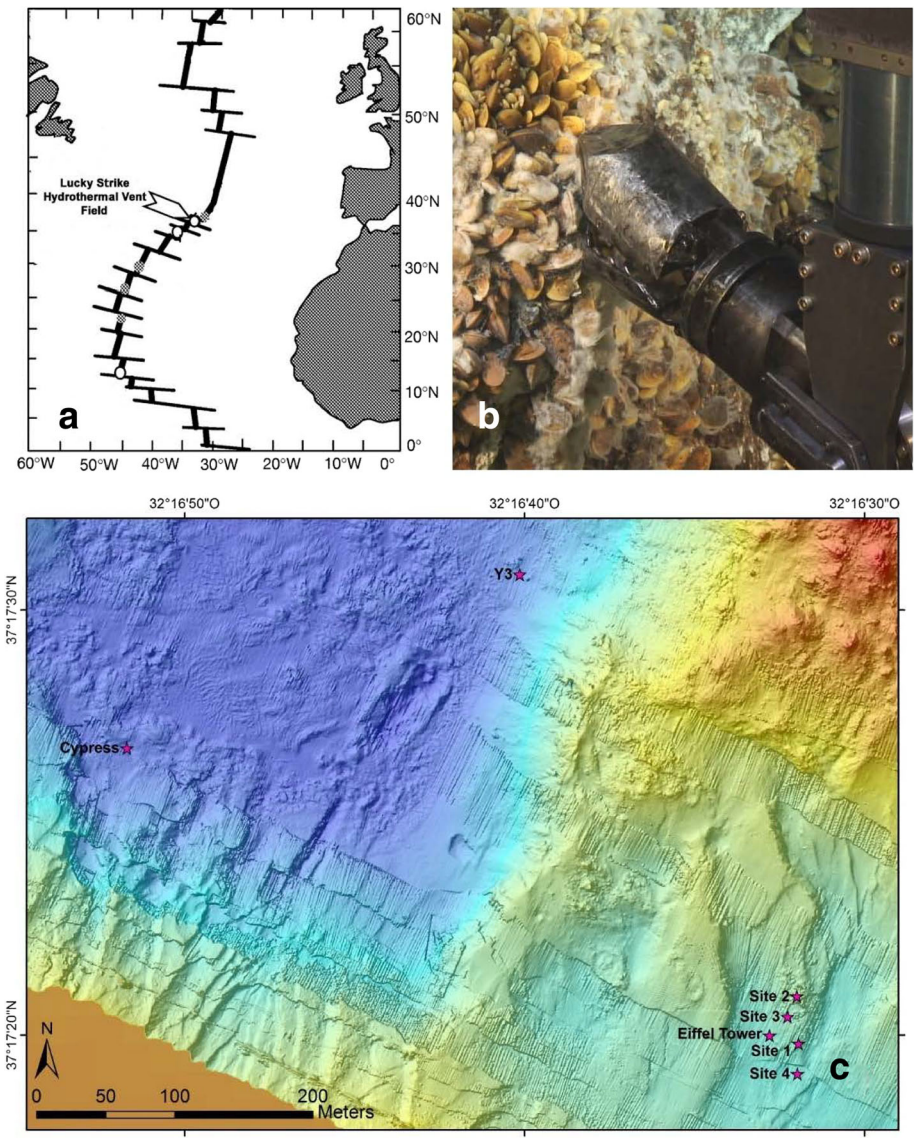

Fig. 1 Study area and sampling sites. **a** Location of the Lucky Strike vent field on the Mid-Atlantic Ridge at 37°17 N, 32°16 W. **b** Samples were collected using the ROV Victor6000 manipulator arm. **c** Locations of the sites where different substrata were deployed around the Eiffel Tower edifice (sites 1, 2, 3 and 4) and sites from which *Bathymodiolus azoricus* assemblages were sampled (Eiffel Tower, Cypress, Y3) are reported

Fig. 5a, b). Nerve ring situated at 337 μm from anterior end (at about 0.4 times oesophagus length from anterior end). Male reproductive system characterized by two testes (anterior testis outstretched, posterior reflected). Spicules equal, 79 μm (2 a.b.d.), slightly ventral curved, with one distally pointed end and one cephalated proximal end (Fig. 2f, g). Two circles of circumcloacal setae (ten pairs of external longer setae and an internal circle of three-four shorter pairs; Fig. 4a, b, c, d). Cloacal aperture surrounded by setae (Fig. 4a, b, c, d). Only one pre-cloacal papilla, post-cloacal papilla absent. Pre-cloacal papilla with four pairs of short stout spines (Fig. 4c, d). Tail conico-cylindrical (Fig. 2f, g; Fig. 4g), 160 μm length (Fig. 4h) with several scattered caudal setae. Spinneret opening in terminal part of tail with one pair of short setae (Fig. 4h).

Females

Very similar to males in appearance, body length up to 8598 μm, maximum body diameter 139 μm (Fig. 2a). No caudal setae. Single anterior ovary, reflexed (Fig. 2b). Gravid female with 2 fertilized eggs (217 μm long). Vulva (Fig. 4e) at 64–69% of body length from anterior end. Demanian system with uvette (connection between main duct and posterior end of uterus) clearly visible (Fig. 5d)

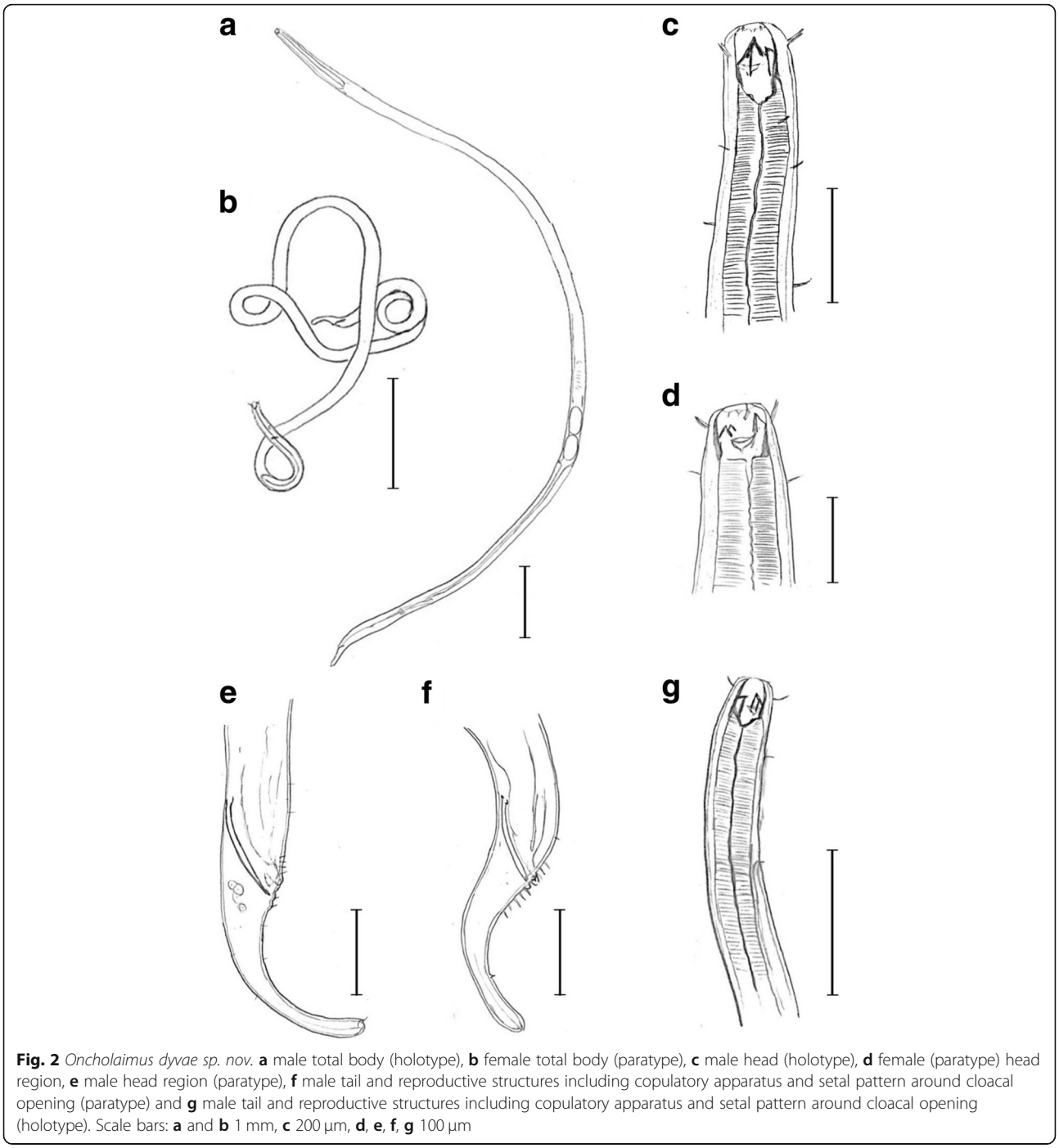

Fig. 2 *Oncholaimus dyvae sp. nov.* **a** male total body (holotype), **b** female total body (paratype), **c** male head (holotype), **d** female (paratype) head region, **e** male head region (paratype), **f** male tail and reproductive structures including copulatory apparatus and setal pattern around cloacal opening (paratype) and **g** male tail and reproductive structures including copulatory apparatus and setal pattern around cloacal opening (holotype). Scale bars: **a** and **b** 1 mm, **c** 200 μm, **d**, **e**, **f**, **g** 100 μm

and connected to exterior through lateral openings or copulation pores (Fig. 4f).

Differential species diagnosis

Oncholaimus dyvae sp. nov. differs from all other members of the genus by the combination of the following characters: body length (up to 9 mm), the presence of a long spicule (79 μm) with a distally pointed end, a complex pericloacal setal ornamentation with one precloacal papilla surrounded by short spines, and a body cuticule with very fine striation shortly posterior to the amphid opening. According to the World Register of Marine Species, *Oncholaimus* accommodates 126 species names of which 85 are considered valid species. These species can be clustered in accordance with their dimensions (most *Oncholaimus* species are less than 5 mm long). Only 19 species are longer than 5 mm (*O. brachycercus* de Man, 1889; *O. chiltoni* Ditlevsen, 1930; *O. cobbi* (Kreis, 1932)

Table 1 Measurements of *Oncholaimus dyvae sp. nov* (in μm)

Characters	Male Holotype	Males Paratype min-max	Females min-max
Total body length	9430	6212–7825	8010–8598
Head diameter	40.0	39–43	44.2–51
Lenght of subcephalic setae	9.0	8–9	9
Lenght of cephalic setae	11.4	10.5–11	11
Amphid fovea height	16.0	15–16	14–15
Amphid fovea width	18.0	17–18	16–17
Amphid fovea width/c.b.d. (%)	38.3	36.6–38.3	35.6–36.9
Nerve ring from anterior end	337	375–380	375–377
Nerve ring c.b.d.	61.5	60–62	60–61
Excretory pore from anterior	172	206–209	250–265
Oesophagus lenght	810	612–915	881–917
Oesophagus c.b.d.	70.3	63–76	76.9–117
Maximum body diameter	95.0	63–90	90–139
Spicule lenght	79	79–101	–
Anal diameter	48.0	40–48	41.2–65
Tail lenght	160	134–165	189–190
Tail lenght/a.b.d.	3.3	2.9–4.1	2.9–4.6
Vulva from anterior	–	–	5130–5912
Vulva c.b.d.	–	–	90–106
V%	–	–	64.1–68.8
a	99.3	98.6–105	61.9–88.9
b	11.6	9–10.2	8.7–9.8
c	58.9	46.4–61.5	42.4–45.3

Rachor, 1969; *O. curvicauda* Allgén, 1957; *O. flexus* Wieser, 1953; *O. lanceolatus* Vitiello, 1970; *O. leptos* Mawson, 1958; *O. longus* (Wieser, 1953) Rachor, 1969; *O. onchorius* Ditlevsen 1928; *O. paraedron* (Mawson, 1958) Rachor, 1969; *O. paraegypticus* Mawson, 1956; *O. plavmornini* Filipjev, 1927; *O. problematicus* Coles 1977; *O. ramosus* Smolanko and Belogurov 1987; *O. scanicus* Allgén, 1957; *O. steinboecki* Ditlevsen, 1928; *O. steineri* Ditlevsen, 1928; *O. thysanouraios* Mawson, 1958; *O. ushakovi* Filipjev, 1927). *O. cobbi*, *O. leptos*, *O. longus* and *O. paraedron* can easily differentiated from the hydrothermal vent species by the presence a ventral papilla on tail (absent in *O. dyvae* sp. nov.). *O. brachycercus*, *O. chiltoni*, *O. flexus*, *O. paraegypticus* and *O. thysanouraios* are characterized by the absence of pre-cloacal papilla (present in *O. dyvae* sp. nov.). *O. curvicauda* is characterized by two crowns of cephalic bristles while *O. dyvae* sp. nov. has ten setae in one circle and the combination of a tail firstly conical (102 μm length) then curved and thin (119 μm length) versus a conico-cylindrical tail (160 μm length) in *O. dyvae* sp. nov. Also *O. plavmornini* has a tail firstly conical then curved and thin (versus the conico-cylindrical tail of *O. dyvae* sp. nov.) and lower a value in males (33–38 versus 99–103 in *O. dyvae* sp. nov.). *O. steinboecki* is characterized by very long and thin tail in males (c 23.6 versus c 46.4–61.5 in *O. dyvae* sp. nov.). *O. ushakovi* has a spicule shorter (52 μm versus 79 μm in *O. dyvae* sp. nov.) without the distally pointed end and the cephalated proximal end typical *O. dyvae* sp. nov.. *O. lanceolatus* has a long and thin tail and differs from *O. dyvae* sp. nov by a, b and c ratio in males (48.5, 6 and 13.9 versus 99.3, 11.6, 58.9).

The remaining five species (*O. onchorius, O. problematicus, O. ramosus, O. scanicus and O. septentrionalis*) differ from *O. dyvae* sp. nov. in finer details reported here below: *O. onchouris* males has distal digitiform tail bent dorsally at an obtuse angle, while *O. dyvae* sp. nov. has a conico-cylindrical tail; *O. problematicus* has straight spicules versus distinctly distally curved spicules in *O. dyvae* sp. nov. together with the absence of pre-cloacal midventral papilla (present in *O. dyvae* sp. nov.; *O. ramosum* has spicules longer (81–198 vs. 79–101 μm) and females, by only two versus numerous copulatory pores in *O. dyvae* sp. nov. and *O. septentrionalis* has shorter (papilliforms) cephalic setae, a slimmer body and longer tail than *O. dyvae* sp. nov. Finally the species most similar to *O. dyvae* sp. nov. is *O. scanicus.* However, both species can be easily differentiated by the absence of a conspicuous pre-cloacal midventral papilla in *O. scanicus*, present in *O. dyvae* sp. nov., the absence of two post-cloacal lateral rows of six short conical elevations in *O. scanicus* present in *O. dyvae* sp. nov. and longer anterior setae in *O. scanicus.* Furthermore, *O. scanicus* has been recorded exclusively in shallow sediments from Öresund, between Demark and Sweden. In contrast to what was reported by Tchesunov [17], which previously identified this hydrothermal vent species as *O. scanicus*, we consider that the severe disparity of habitats, together with evident morphological differences (conspicuous pre-cloacal midventral papilla, two post-cloacal lateral rows of six short conical elevations) are strong characters to separate these species.

DNA taxonomy

The maximum likelihood (ML) tree shows that *Oncholaimus dyvae* sp. nov. forms a clade and clusters with *Oncholaimus* sp. (accession numbers HM564402, HM564475, AY854196, LC093124, KR265044), *Viscosia* sp. (accession number FJ040494) and other Oncholaimidae (accession number KR265043, FJ040493, AY866479, HM564620, HM564605) (Fig. 6). The genera *Oncholaimus* seems to be polyphyletic, but this is maybe due to artefactual misidentification of specimens. The sister group of the new species is not clear because of a poor support and resolution. Moreover, it should be stressed that very few species of Oncholaimoidea are represented in GenBank. DNA taxonomy through Poisson Tree Process (PTP) provides a total of 29 units (from ML solution) and 30 units (from

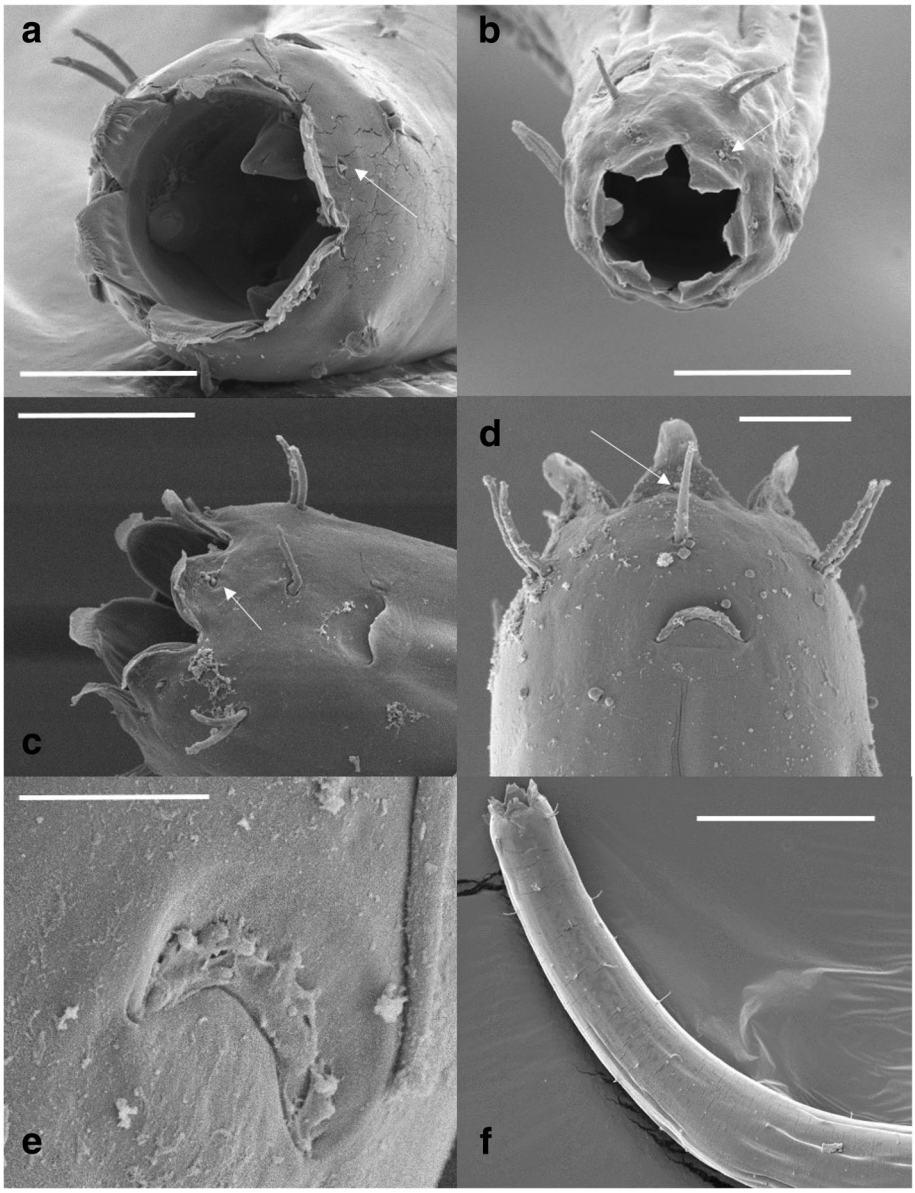

Fig. 3 Scanning electron micrographs of *Oncholaimus dyvae* sp. nov. anterior body (**a**) buccal cavity with view on teeth with openings of pharyngeal glands (front view), **b** head (apical vision), **c**,**d**) head lateral visions, minute rounded inner labial papillae are indicated by arrows (**a**,**b**,**c**,**d**), **e** amphid opening with corpus gelatum, **f** anterior body (lateral view). Scale bars: **a**, **b** and **c** 20 μm, **d** 10 μm, **e** 5 μm, **f** 100 μm

Bayesian solution) and corroborates the fact that all the individuals of *O. dyvae* sp. nov. belong to one single species, which is also different from any other species already present in GenBank (Fig. 6).

Oncholaimus dyvae sp. nov. abundance and biomass

No *Oncholaimus dyvae* sp. nov. was recorded from the organic and inorganic substrata located at site 4 (a sediment area located between the Eiffel Tower and Montsegur edifices), and very low abundance and biomass were reported at site 1 (4.39–5.78 ind/m^2 and 13.38–17.63 μgC/m^2; Table 2). Regarding the colonization experiment, the highest abundance and biomass of *O. dyvae* sp. nov. were reported on the wood located at the highest vent emission site (B2), where *O. dyvae* sp. nov. reached 757.64 ind/m^2 and 2311.15 μgC/m^2. *O. dyvae* sp. nov. was encountered in all *Bathymodiolus* assemblages investigated, reaching the highest abundance and biomass values at the Eiffel Tower site (3290 ind/m^2 and 141,470 μgC/m^2). Abundance of *O. dyvae* sp. nov. differed between the substrata (nested ANOVA: $F_{2,4} = 9.3$, $p = 0.031$), with *Bathymodiolus* assemblage having higher abundance than bone and slate, and partially overlapping with wood (Fig. 7a). Regarding the effect of temperature, a quadratic relationship

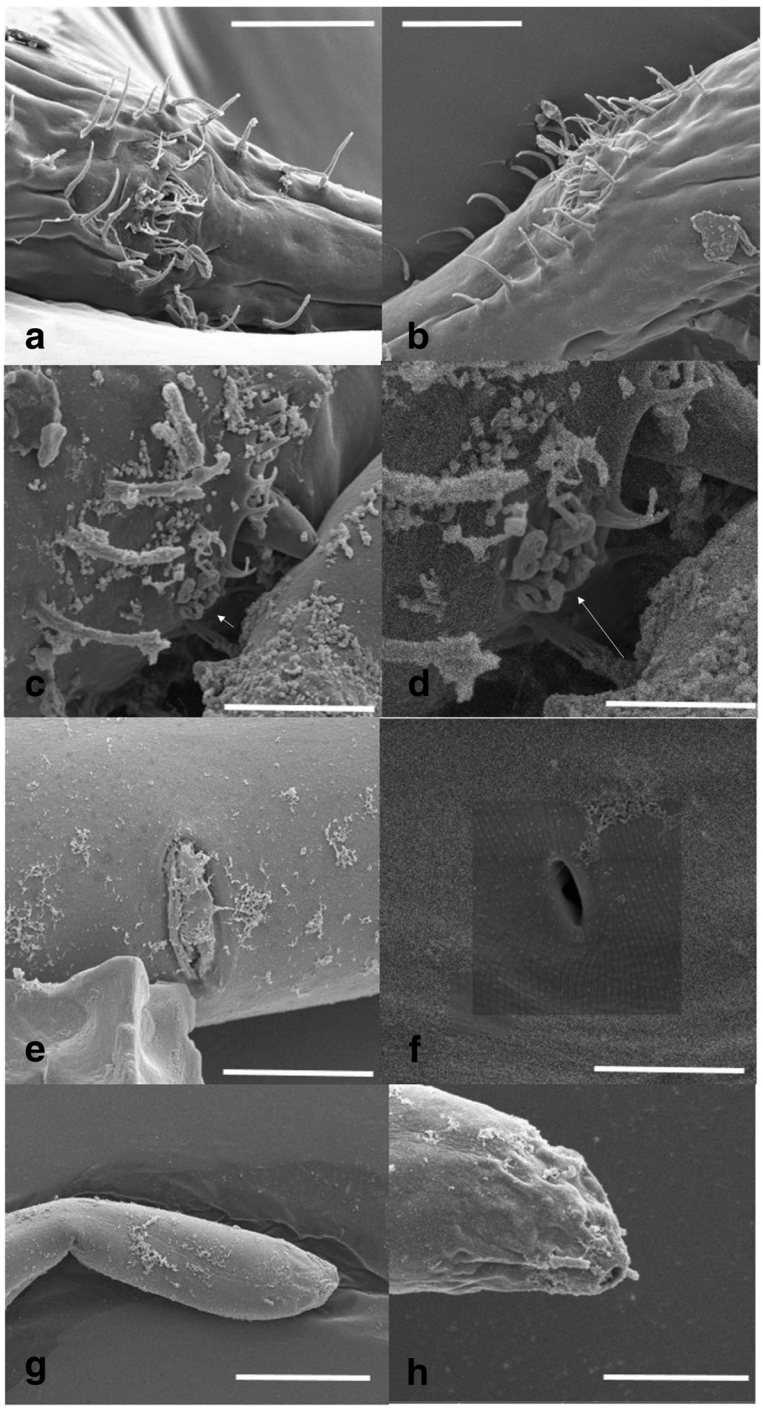

Fig. 4 Scanning electron micrographs of *Oncholaimus dyvae* sp. nov. male and female secondary sexual features. **a**,**b** complex cloacal ornamentation in male with precloacal setae, precloacal papilla, fringe, spicule's tips, **c**,**d** precloacal papilla (indicated by arrows) in male with 4 pairs of short, stout spines, **e** copulatory pore (vulva) in female, **f** lateral opening in female connected to the Demanian system, **g** tail tip, **h** caudal pore of the spinneret. Scale bars: **a**, **b** and **e** 20 μm, **c** and **h** 10 μm, **e** 5 μm, **g** 30 μm

(adjusted $R^2 = 0.84$) fitted the data better (ANOVA: $p = 0.05$) than a linear relationship (adjusted $R^2 = 0.66$) (Fig. 7b), and revealed a significant effect of temperature ($F_{2,4} = 17.4$, $p = 0.011$).

Carbon and nitrogen stable isotope ratios

In all three Eiffel Tower samples, *Oncholaimus dyvae* sp. nov.'s $\delta^{15}N$ was lower than the one of photosynthetic-derived organic matter (Table 3, Fig. 8), and markedly

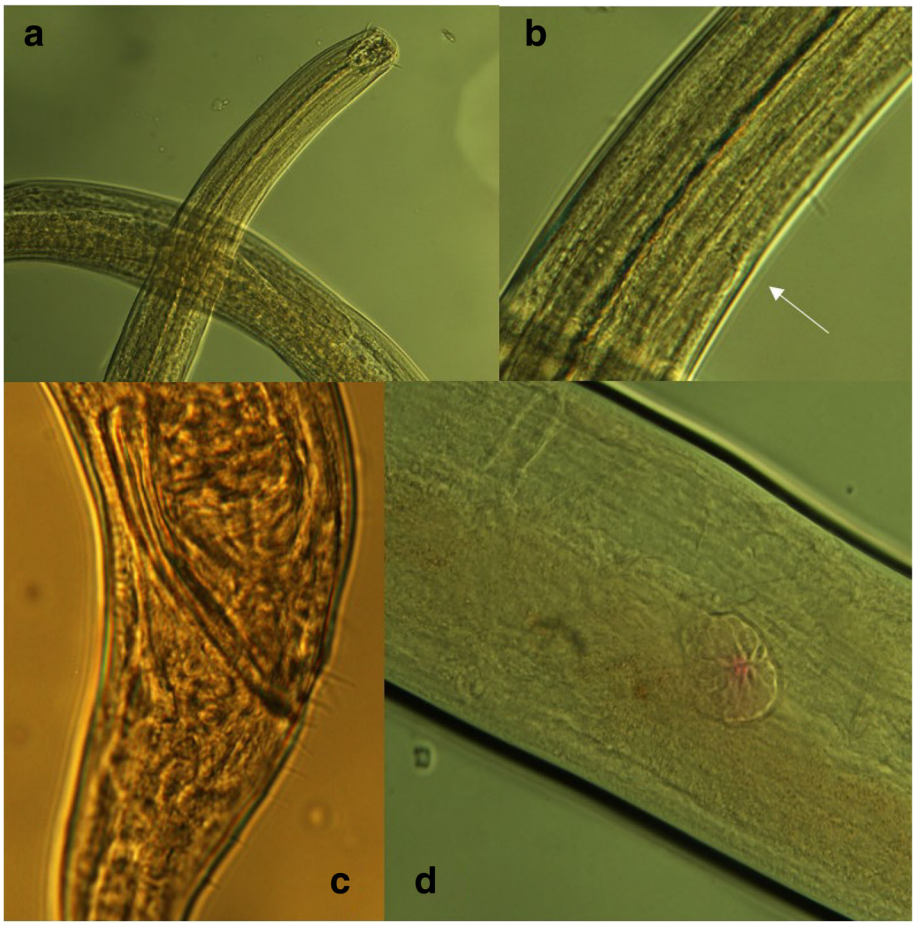

Fig. 5 Light micrographs of *Oncholaimus dyvae* sp. nov. **a** anterior part of the body, **b** detail of the outlet of the secretory-excretory system with ampulla (indicated by an arrow), **c** male spicule, **d** part of the Demanian system (uvette) in female

higher than the one of *Bathymodiolus azoricus* tissues (over 12‰; Table 3, Fig. 8). $\delta^{15}N$ values of *O. dyvae* sp. nov. were 3.9 to 5.8 ‰ higher than those of *Beggiatoa* bacterial mats. Moreover, analysed *O. dyvae* sp. nov. specimens were clearly more ^{13}C-enriched than *Beggiatoa* mats or *B. azoricus* tissues (up to 6 ‰, Table 3). Interestingly, isotopic ratios of *O. dyvae* sp. nov. fluctuated from one sample to another, and those fluctuations closely matched those of their bivalve hosts (Table 3, Fig. 8), as shown by almost identical net differences between *O. dyvae* sp. nov. and *B. azoricus* muscle for both isotopic ratios and in all 3 samples (Table 3).

Discussion

Ecology of Oncholaimus dyvae sp. nov. in deep-sea hydrothermal vents

Species of *Oncholaimus* have been reported around the world in association with shallow-water hydrothermal vents (3 m water depth; [19]). Some *Oncholaimus* species tolerate extreme geothermal and hypersaline conditions as well as high sulfur concentrations. One example is the species *Oncholaimus campylocercoides* found in hydrothermal sources of the Aegean, Baltic and North Seas [20]. This species can produce secretions containing sulfur when exposed to hydrogen sulfide, thereby potentially reducing its toxicity. It was hypothesized that the accumulation of elementary sulfur also provides an energy "reserve" for subsequent oxidation into thiosulfate, sulfite, or sulfate in normoxic conditions [20] although no evidence has been provided so far.

To date, large nematodes belonging to *Oncholaimus* have rarely been reported from deep-sea hydrothermal vents [13, 17]. The genus *Oncholaimus* was for the first time reported in very high abundance at the Lucky Strike vent field [10]. Also Tchesunov [17] reported *Oncholaimus* from two other deep-sea hydrothermal vents of the Atlantic Ocean (Menez Gwen and Lost City, Mid Atlantic Ridge). In the present study, we reported a high density of *Oncholaimus* and we describe the new species *Oncholaimus dyvae* sp. nov. from the organic colonization substrata deployed

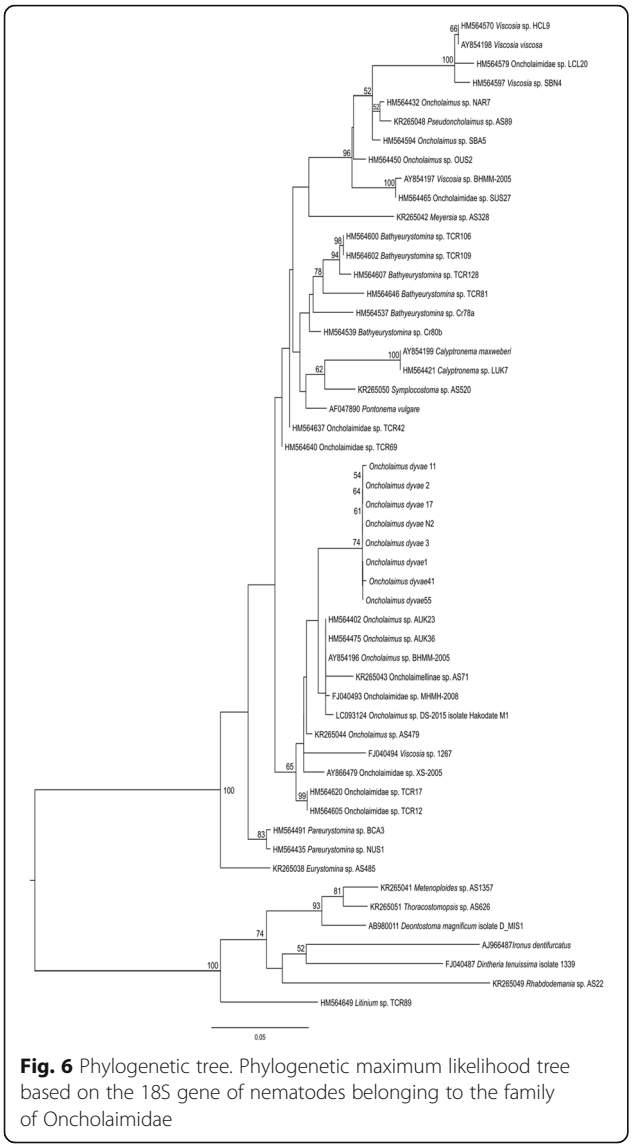

Fig. 6 Phylogenetic tree. Phylogenetic maximum likelihood tree based on the 18S gene of nematodes belonging to the family of Oncholaimidae

Table 2 *Oncholaimus dyvae* sp. nov. abundance and biomass (*A* slate, *B* wood, *C* bone, *CY* Cypress, *ET* Eiffel Tower)

Sample	Abundance (ind/m^2)	Biomass (μgC/m^2)
A2	11.40	34.77
A3	66.21	201.96
A1	5.78	17.63
A4	0	0
B2	757.64	2311.15
B3	0	0
B1	4.39	13.38
B4	0	0
C2	14.29	43.58
C3	60.87	185.68
CY	127.50	548.30
Y3	392.50	1687.80
ET	3290.00	14,147.00

at the most active sites around the Eiffel Tower [10]. We also reported *Oncholaimus dyvae* sp. nov. in very high abundance associated with *Bathymodiolus* assemblages at Eiffel Tower while their abundances were much lower at Cypress and Y3. Overall, *O. dyvae* sp. nov. abundance increased with higher temperature and vent emission (Fig. 7) and no individual was found at the inactive colonization site (Table 2). Such data seems to indicate that the distribution of *O. dyvae* sp. nov. is linked with the presence of hydrothermal activity although not at all active sites. Indeed, in a recent paper on Eiffel Tower faunal assemblages, no *Oncholaimus* was reported from the 12 sampling units [9]. However, the presence of another genus belonging to the family Oncholaimidae (*Viscosia*) was reported in one of their samples [9]. In terms of biomass, our values are several orders greater than deep-sea nematode fauna, but comparable to the Condor seamount nematofauna, where high nematode biomass values (due to the presence of large Comesomatidae nematodes) were recorded at the seamount bases [21].

Trophic ecology of Oncholaimus dyvae sp. nov.

The δ^{15}N of *Oncholaimus dyvae* sp. nov. was lower than the one of photosynthetic-derived organic matter. While this food source could partly contribute to nematode diet, it is therefore unlikely to be a major food item. Moreover, despite the fact that *O. dyvae* sp. nov. was found in extraordinarily high densities associated to *Bathymodiolus azoricus*' byssus, the very substantial δ^{15}N difference (over 12‰) between the nematode and its bivalve host rules out the existence of a direct trophic link between them. We can hypothesize that the byssus could act as shelter offering camouflage and protection from predation or simply as a physically suitable three-dimentional substratum in an environment where most substrates are bare (i.e. no sediment), particularly near the vents and sources of emissions. In addition, the byssus may act as a trap for organic matter. Nitrogen stable isotope ratios suggest that *Beggiatoa* bacterial mats could constitute a feasible food source for *O. dyvae* sp. nov. Moreover, δ^{13}C and δ^{15}N of *O. dyvae* sp.nov. were comparable with those of other detritivore animals sampled at the Lucky Strike vent, such as the polychaete *Amphisamytha lutzi*, or the gastropods *Protolira valvatoides* and *Pseudorimula midatlantica* [22]. The fact that fluctuations in stable isotope ratios of C and N in *O. dyvae* sp. nov. closely match those observed in the tissues of

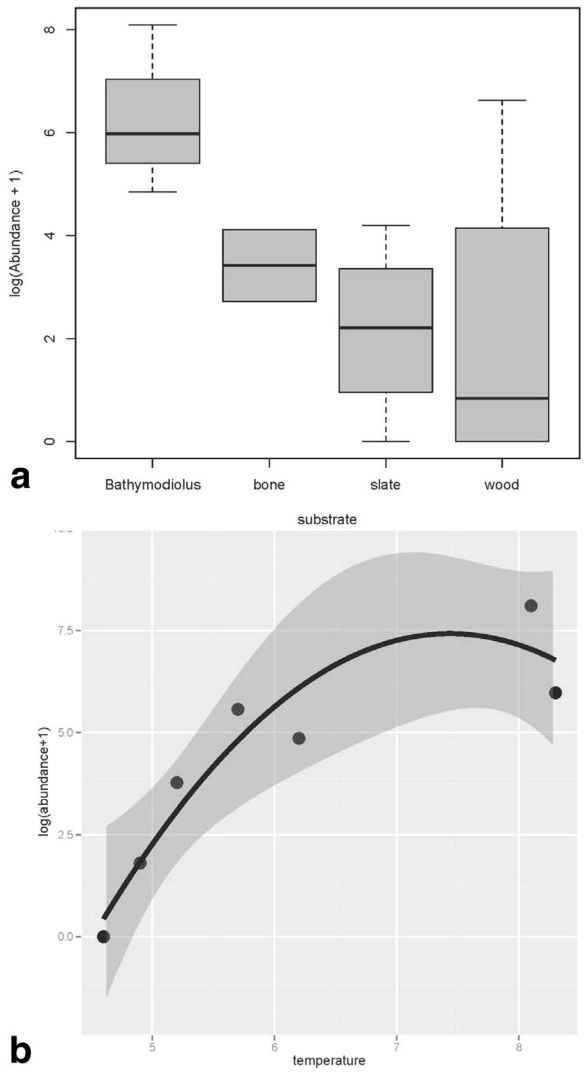

Fig. 7 Relationship between *Oncholaimus dyvae* sp. nov. abundance and environmental conditions. **a** Relationship between *Oncholaimus dyvae* sp. nov. abundance (expressed in logarithmic scale) and substratum. **b** Relationship between *Oncholaimus dyvae* sp. nov. abundance (expressed in logarithmic scale) and habitat temperature for each of the seven analysed sites, including model fit with 95% confidence interval

endosymbiotic mussels *B. azoricus* could nevertheless indicate that some kind of nutritional relationship exists between the nematode and its bivalve host. The nature of this relationship remains an open question, but could involve the nematode feeding on bivalve-associated bacteria. These results, together with the fact that no potential preys were identified in the surrounding food web [22], suggest that *O. dyvae* sp. nov. is a detritivore/bacterivore, which partly relies on free-living chemoautotroph microbes. Moreover, *O. dyvae* sp. nov.'s $\delta^{13}C$ was clearly higher than *Beggiatoa mats* or *B. azoricus* tissues. This clearly indicates that CBB thiotrophs are not the nematode's sole food source. It could instead rely on a mix of thiotrophs and methanotrophs micro-organisms, explaining its intermediary $\delta^{13}C$ values. Furthermore, sulfur-oxidizing bacteria related to Epsilonproteobacteria and Gammaproteobacteria were detected in the cuticle, in the digestive cavity and in the intestine of *O. dyvae* sp. nov. suggesting a potential symbiotic association [23].

More research is needed to evaluate the relative importance of both of these groups in the nematode diet. The polynoid annelid *Branchinotogluma mesatlantica* has been identified as a potential predator of *O. dyvae* sp. nov. (unpublished data), but more evidence is needed to validate this hypothesis. As recently shown for *Oncholaimus moanae*, nematodes can be a high quality food source to predators thanks to their high amount of highly unsaturated fatty acids (HUFAs) [24]. In the deep sea and hydrothermal vents, such source may play an even more important role for food webs as basal sources have usually low amount of HUFAs [25, 26]. Unlike most metazoans, nematodes have been shown to be able to biosynthesize HUFAs from acetate [27, 28]. Often neglected for their size, nematodes can thus represent an important trophic component of vent communities.

Conclusions

This study improves our understanding of vent biology and ecology, revealing a new nematode species able to adapt and be very abundant in active vent areas due to their association with chemosynthetic micro-organisms. Faced by the

Table 3 Stable isotope ratios (expressed in ‰) of microbial mats, tissues of *Bathymodiolus azoricus* and *Oncholaimus dyvae* sp. nov. nematodes at the Eiffel Tower (ET1, ET2 and ET3). Standard deviations are given in parentheses. $\Delta_{Oncholaimus\ -\ muscle}$ represents the net difference of isotopic ratios between *O. dyvae* sp. nov. and *B. azoricus* muscle

	ET1			ET2			ET3		
	$\delta^{13}C$	$\delta^{15}N$	n	$\delta^{13}C$	$\delta^{15}N$	n	$\delta^{13}C$	$\delta^{15}N$	n
Beggiatoa sp_mat	−32.6 (0.6)	−2.5 (0.1)	2						
B. azoricus gill	−30.6 (1.0)	−12.7 (1.3)	5	−25.4 (4.2)	−10.3 (2.1)	4	−31.4 (0.6)	−12.2 (1.0)	4
B. azoricus byssus	−27.6	−10.1	1						
B. azoricus muscle	− 30.4 (0.9)	−11.0 (1.6)	5	−28.4 (1.3)	−9.1 (0.5)	4	−31.3 (0.6)	−11.1 (0.3)	4
Oncholaimus dyvae sp. nov.	−24.7	1.9	1	−22.8	3.3	1	−25.3	1.4	1
$\Delta_{Oncholaimus\ -\ muscle}$	5.7	12.9		5.6	12.4		6.0	12.5	

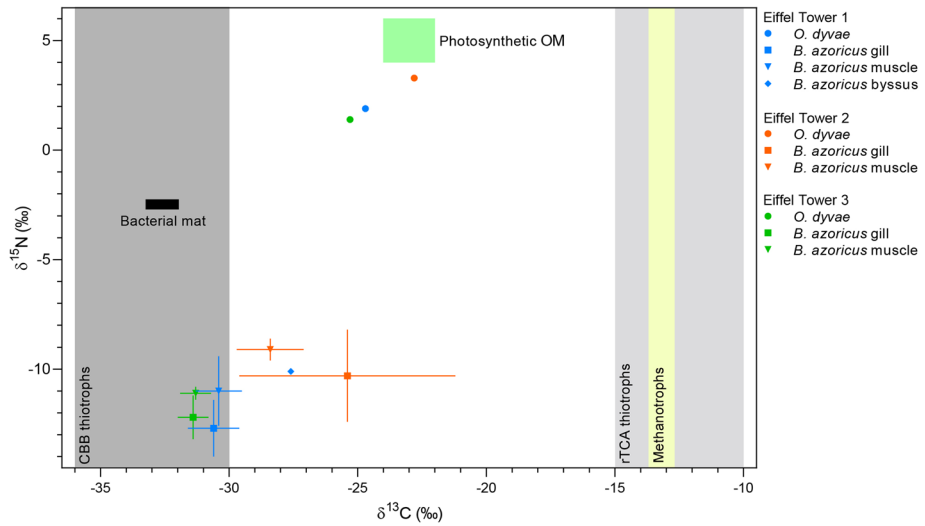

Fig. 8 Biplots of carbon ($\delta^{13}C$) and nitrogen ($\delta^{15}N$) signatures. Biplots of $\delta^{13}C$ and $\delta^{15}N$ signatures (mean ± SD, expressed in ‰) of *Oncholaimus dyvae* sp. nov., *Bathymodiolus azoricus* (gill, muscle and byssus) and potential basal sources in Eiffel Tower

rapid increase of anthropogenic pressure to access mineral resources in the deep sea, hydrothermal vents are particularly susceptible to be impacted by exploitation of seafloor massive sulfide deposits [29]. It is necessary to document and understand vent species able to flourish in these peculiar ecosystems.

Methods

The study area and sampling collection

The Lucky Strike vent field is situated on the Mid-Atlantic Ridge, south of the Azores (Table 4 and Fig. 1). This vent field is composed by three volcanic cones enclosing a lava lake (with a diameter of 200 m [30]). It hosts around 20 active edifices including "named as" Eiffel Tower, Cypress and Y3. Eiffel Tower and Y3 can be found on the eastern side of the field, while Cypress is located on its western side. Eiffel Tower is an active edifice characterized by an eight of 11 m. In the Lucky Strike vent field, Eiffel Tower is the most studied edifice.

Samples were collected during three oceanographic cruises: Momarsat 2011 (29/06–23/07/2011), Biobaz 2013 (2–20/08/2013) and Momarsat 2014 (13–31/07/2014) on the research vessel "*Pourquoi Pas*? ". Sample collection was carried out using the remotely operated vehicle (ROV) Victor6000. During the Momarsat 2011 cruise, samples for nematode morphological identification, abundance and biomass analyses were collected from inorganic (slates reported as A), and organic (woods reported as B and bones reported as C) colonisation substrata [10]. At the Eiffel Tower we performed a long-time experiment involving the deployment of these substrates at increasing distances from inactive to active hydrothermal vent are (Sites 1, 2, 3, 4, see details in [10]). The sites less active were site 1 (3 m from the edifice) and 3 (4–5 m from the edifice) located at the base south of the Eiffel Tower. Site 1 was caracterized by very few organisms while site 3 was on a crack with diffuse venting, where *Bathymodiolus azoricus* mussels and microbial mats were recorded. The most active site was site 2 located on the north-west flank of Eiffel Tower and near to fluid exits surrounded by dense Bathymodiolus azoricus assemblages. Site 4 was an external sedimentary site located between the Eiffel Tower and Montségur edifices. The other nematode samples came from a broad-scale study on the structure of *Bathymodiolus azoricus* assemblages at Lucky Strike initiated by Sarrazin et al. in 2012 (unpublished data) (Table 4 and Fig. 1). These assemblages were collected from the Eiffel Tower, Y3 and Cypress edifices

Table 4 Location, depth and temperature measured on the substratum and within the mussel assemblages at the different sampling sites. Fluid inputs in percentage were calculated using the formula provided by Sarradin et al. [2] for the Eiffel Tower edifice (% = 0.314 T – 1.38). *CY* Cypress, *ET* Eiffel Tower

Site	Latitude	Longitude	Depth	T°C			% fluid
	(N)	(W)	(m)	Average	Min	Max	inputs
2	37° 17.3484′	32° 16.5333′	1699	5.7	4.3	7.7	0.41
3	37° 17.3404′	32° 16.5379′	1698	5.2	4.4	6.7	0.25
1	37° 17.3299′	32° 16.5325′	1704	4.9	4.3	6.7	0.16
4	37° 17.3181′	32° 16.5331′	1705	4.6	4.3	4.9	0.06
CY	37° 17.4458′	32° 16.8617′	1739	6.2	4.8	7.6	0.57
Y3	37° 17.5138′	32° 16.6691′	1728	8.3	4.4	12.2	1.23
ET	37° 17.3330′	32° 16.5467′	1692	8.1	3.8	12.4	1.16

(Table 4 and Fig. 1) during Biobaz 2013 and Momarsat 2014 cruises. The fauna was sampled using Victor's suction sampler and arm grab following the protocol described in Cuvelier et al. [31]. Once brought on board, faunal samples from each location were washed over stacked sieves (1 mm, 250 μm and 63 μm mesh size) and stored with filtered seawater at 4 °C temperature. *Bathymodiolus* specimens were individually carefully washed over sieves and, together with the sieves, byssus was checked at stereomicroscope.

Nematode sorting and fixation

Nematodes were sorted directly on board of the research vessel under a stereomicroscope from the colonisation substrata or from the mussel assemblages. We selected one of the most abundant species (previously identified as *Oncholaimus* sp.1 [10]). Due to its size (several millimeters), the species could easily be separated from the other species directly at the stereomicroscope. A set of specimens was fixed in 4% formaldehyde for morphological description. Another set of individuals was immediately frozen at − 80 °C for molecular and stable isotope analyses. Other individuals were prepared for Scanning Electron Microscopy (SEM) studies: nematodes were fixed in 2.5% glutaraldehyde for 16 h at 4 °C, then transferred in a sodium azide solution (0.065 g in 150 ml filtered sea water) and stored at 4 °C until use.

Nematode morphological analysis

In order to confirm that all nematodes were conspecific, we performed a detailed morphological examination for a subset of the population. Several nematodes were mounted on slides for detailed morphological observations using the formalin-ethanol/glycerol method [32, 33]. Drawings and photos were made with a Leica DM IRB inverted light microscope equipped with live-camera (Image-Pro software) and on Zeiss AxioZoom microscope equipped with live-camera (Zen software). Type material is deposited in the Natural History Museum of Denmark (holotype NHMD-115822, paratypes from NHMD-115823 to NHMD-115832). This species is deposited in ZooBank with accession number urn:lsid:zoobank.org:pub:38105B1C-9E7D-42FD-BF74-D403218D12A5. Specimens chosen for scanning electron microscopy were transferred to a 0.8% osmium tetroxide solution for 20 h, then gradually transferred to pure ethanol using a graded ethanol series (10, 25, 40, 60, 80%, 90, 100%,15 min each), critical point dried, and mounted onto stubs before coating with gold (about 15-20 nm thickness) using a sputter coater. Nematodes were studied with the scanning microscope FEI QUANTA 200 at 5.00 kv voltage.

Nematode DNA extraction, PCR, and sequencing

As an additional control to check that all nematodes in the population with the same morphology indeed belonged to the same species, we used a DNA taxonomy approach based on DNA sequence data from 42 individuals. DNA extraction was performed with Chelex®. Each nematode was first incubated in 35 μl in a 5% Chelex® solution supplemented with 1 μl of proteinase K for 1 h at 56 °C followed by 20 min at 95 °C. The sample was then vortexed for 15 s: the Chelex® solution contains styrene-divinylbenzene beads that help grind the tissues and release DNA. The samples were centrifuged and the supernatants were recovered and stored at − 20 °C.

The polymerase chain reaction (PCR) amplifications for 18S rDNA (the small subunit of ribosomal DNA) and for 28S rDNA (the large subunit of ribosomal DNA) were carried out in a final volume of 25 μl using following mix: 2 μl of extracted DNA was added to 5 μl of 5x PCR buffer and 0.1 μl Taq polymerase (5 U/μl - Promega). For the 18S rRNA, 10 mM of each dNTP, 62.5 mM of $MgCl_2$ and 10 μM of each of the two primers were added. For the 28S rDNA, 5 mM of each dNTP, 50 mM of $MgCl_2$ and 20 μM of each of the two primers were added. The following primers were used: 18S1.2a (5′ – CGATCAGATACCGCCCTAG – 3′), 18Sr2b (5′ – TACAAAGGGCAGGGACGTAAT– 3′)), D2Ab (5′-ACAAGTACCGTGAGGGAAAGTTG-3′) and D3B (5′-TCGGAAGGAACCAGCTACTA-3′). The PCR cycles were 2 min at 94 °C then 30 cycles of 1 min denaturation at 94 °C, 1 min annealing at 55 °C and 2 min extension at 72 °C, followed by 10 min at 72 °C. All amplification products were run on a 0.8% agarose gel to verify the size of the amplicons. Then, 20 μl of each PCR product were sent to GATC Biotech for sequencing. Each nematode was sequenced in both forward and reverse direction. We could obtain 18S sequences (592 bp) for 40 of the 42 animals and 2 sequences of 28S (607 pb). Chromatograms were checked using the FinchTV software package (©Geospiza Inc.), and all sequences were deposited in GenBank with accession number from KY451633 to KY451672.

DNA taxonomy

We aimed at testing whether the new morphologicaly identified species could be supported as one unique molecular evolutionary entity and second to test their novelty with available sequences (NCBI database). In order to achieve this, we used a DNA taxonomy approach [34], namely the Poisson Tree Process (PTP [35]). All 18S sequences belonging to the superfamily Oncholaimoidea were retrieved, belonging to 13 named genera. Only five sequences are identified to species level, corresponding to three species: *Calyptronema maxweberi*, *Pontonema vulgare* and *Viscosia viscosa*. All sequences present in NCBI overlapping with the amplified fragment were used in the analysis. In order to eliminate redundancy, if some sequences were identical to

Table 5 Isotope signature estimates for the potential dominant basal sources in the Lucky Strike vent field

Basal sources	$\delta^{13}C$	$\delta^{15}N$	Reference
Photosynthetic_derived OM	−24 to −22 ‰	4–6‰	Gebruk et al. [42]; Khripounoff et al. [43]
Methanotrophs (methane $\delta^{13}C$)	−13.7 to −12.7 ‰	Low or negative	Charlou et al. [44]
Thiotrophs using the rTCA cycle	−15 to −10 ‰	Low or negative	Hügler & Sievert [45], Sievert et al. [46]
Thiotrophs using the CBB cycle	−36 to −30 ‰	Low or negative	Hügler & Sievert [45], Sievert et al. [46], Trask & Van Dover [47]

others, we selected only one for each group of identical sequences. Also, for the putative new species, we reduced the dataset to unique sequences only. All unique non-redundant sequences were aligned using MAFFT [36] with Q-Ins-i settings, suitable for ribosomal markers. To perform PTP [35], we used as input a maximum likelihood (ML) reconstruction in RAxML 8.2.2 (Randomized Axelerated Maximum Likelihood [37]). The alignment for RAxML included also seven outgroup sequences from closely related nematode groups: *Dintheria tenuissima* (Bastianiidae), *Deontostoma magnificum* (Leptosomatidae), *Ironus dentifurcatus* (Ironidae), *Litinium* sp. (Oxystominidae), *Rhabdodemania* sp. (Rhabdodemaniidae) and *Metenoploides* sp. and *Thoracostomopsis* sp., (Thoracostomopsidae). We used GRT + G + I as evolutionary model, with 500 bootstrap resampling. The outgroups were then removed before performing PTP.

Nematode biomass

The nematode biomass was calculated from the biovolume of all the individuals collected per replicate using the Andrassy formula ($V = L \times W^2 \times 0.063 \times 10^{-5}$, where V is expressed in nL (10^{-9} L) with body length, L, and width, W, expressed in μm [38]). The carbon contents were identified as representing 40% of the dry weight [39]. From each sample, 200 collected nematodes were isolated using an AxiozoomV16 stereomicroscope (400× magnification) using the software Zen 2012 (blue edition). We did not perform any test on biomass values, similar to what we did for abundance values, given that biomass was strictly correlated to abundance (Pearson's correlation r = 0.99).

Statistical analyses

We tested whether the abundance of the investigated nematode species was influenced by substratum and by temperature. For the effect of substratum, a categorical variable with four levels, slate, wood, bone, or *Bathymodiolus*, sampled in different sites, was used as an explanatory variable in a nested Analysis of Variance (ANOVA): given the inherent pseudo replication in the sampling design, we included the confounding effect of site in the random structure. For the effect of temperature, we removed the confounding effect of site by averaging abundance values for each site before performing the test. We then tested, using ANOVA test between models, whether a linear or a quadratic relationship between abundance and average temperature for each site could be a better fit to the data. All tests were run in R 3.1.2 [40], and abundance data were used in the models after logarithmic transformation.

Carbon and nitrogen stable isotopes ratios

We studied feeding ecology of the selected nematode species by analyzing carbon and nitrogen stable isotope ratios. On board, *Bathymodiolus azoricus* mussels (gill, muscle and byssus), filamentous bacterial mats as well as nematode individuals from the different species associated with *Bathymodiolus* were frozen (− 80 °C) for isotopic analyses. In the laboratory, samples were rinsed, after fixation, in distilled Milli-Q water. For nematodes, the whole body was used and several animals were pooled to reach the minimum weight required for stable isotope analyses (10 to 20 nematodes per sample). Samples were freeze-dried and ground into a homogeneous powder using a ball mill. Tissue was precisely weighed (0.4 ± 0.1 mg) in tin capsules. Samples were analysed on a Flash EA 1112 elemental analyser coupled to a Thermo Scientific Delta V Advantage stable isotope ratio mass spectrometer (EA-IRMS). Analytical precision based on the standard deviation of replicates of internal standards was ≤0.1‰ for both $\delta^{13}C$ and $\delta^{15}N$. Values are expressed in δ (‰) notation with respect to VPDB ($\delta^{13}C$) and atmospheric air ($\delta^{15}N$): $\delta X\ (‰) = [(R_{sample} / R_{standard}) - 1] \times 10^3$, where X is either ^{13}C or ^{15}N, R_{sample} is the $^{13}C/^{12}C$ or $^{15}N/^{14}N$ isotope ratio in the sample and $R_{standard}$ is the $^{13}C/^{12}C$ or $^{15}N/^{14}N$ isotope ratio for the VPDB standard ($\delta^{13}C$) or atmospheric air ($\delta^{15}N$).

Isotopic ratios of nematodes were compared to those of potential food items from *B. azoricus* assemblages (Table 5), including filamentous bacterial mats that are dominated by *Beggiatoa (Gammaproteobacteria,* [41]), *B. azoricus* tissues and several chemosynthetic microorganisms groups (Table 5).

Abbreviations

a (de Man index): body length/maximum body diameter; a.b.d.: anal body diameter; b (de Man index): body length/oesophagus length; c (de Man index): body length/tail length; c.b.d: corresponding body diameter; V: vulva distance from anterior end of body; V%: distance of vulva from anterior end × 100 / body length

Declarations

Acknowledgements
We thank the chief scientists, the scientific party and the crew of R/V *Pourquoi pas*? and Victor6000 pilots during the cruises Momarsat 2011 (DOI https://doi.org/10.17600/11030070), BIOBAZ (DOI https://doi.org/10.17600/11030100) and Momarsat 2014 (DOI https://doi.org/10.17600/14000300) for support during the sampling. Authors thank Julie Tourolle for helping in performing study area map and Erwann Legrand for helping in sorting nematodes.

Authors' contributions
DZ, MACB and JS conceived the study; DZ, NG, MP, J S and MACB collected samples; LB, DF, SF and PM performed DNA taxonomy on nematodes; DZ, WD, NS, MS. and AV conducted nematode morphological descriptions; DF did the statistical analyses; LM and MP performed isotopic analyses; DZ, LB, MACB, WD, DF, SF, NG, PM, LM, MP, NS, MS, AV and JS wrote the paper. All authors read and approved the final manuscript.

Funding
This study (the design of the study, collection, analysis, interpretation of data and in writing the manuscript) was supported by the project "Deep-sea hYdrothermal Vent nematodes as potential source of new Antibiotics" (DYVA) and by the project "Prokaryote-nematode Interaction in marine extreme envirOnments: a uNiquE source for ExploRation of innovative biomedical applications" (PIONEER) both funded by the Total Fondation and Ifremer. The collection of data of this work is in the framework of the EMSO-Açores observatory whose research is supported by a grant from the French Government (ANR LuckyScales ANR-14-CE02–0008-02). D.Z. (interpretation of data and writing the manuscript) was partly supported by the "Laboratoire d'Excellence" LabexMER (ANR-10-LABX-19), co-funded by a grant from the French government under the program "Investissements d'Avenir" by a grant from the Regional Council of Brittany (SAD programme). D.Z. also gratefully acknowledges the SYNTHESYS EC-funded project by providing grant to access to the Natural History Museum of Denmark (taxonomical identification). DF thanks the EGIDE-CAMPUS France grant for support during his visiting fellowship at Ifremer (molecular analysis).

Availability of data and materials
Type material is deposited in the Natural History Museum of Denmark (holotype NHMD-115822, paratypes from NHMD-115823 to NHMD-115832). This species is deposited in ZooBank with accession number urn:lsid:zoobank.org:pub:38105B1C-9E7D-42FD-BF74-D403218D12A5. All sequences were deposited in GenBank with accession number from KY451633 to KY451672.

Ethics approval and consent to participate
Not applicable.

Consent for publication
Not applicable.

Competing interests
The authors declare that they have no competing interests.

Author details
[1]IFREMER Centre Brest REM/EEP/LEP, ZI de la pointe du diable, CS10070, 29280 Plouzané, France. [2]IFREMER, Centre Brest UMR 6197 - Laboratoire de Microbiologie des Environnements Extrêmes (REM/EEP/LM2E), ZI de la pointe du diable, CS10070, 29280 Plouzané, France. [3]CNRS UMR 6197-Laboratoire de Microbiologie des Environnements Extrêmes (LM2E), Institut Universitaire Européen de la Mer (IUEM), Technopole Brest-Iroise, Plouzané, France. [4]Université Bretagne Occidentale (UBO), UMR 6197 - Laboratoire de Microbiologie des Environnements Extrêmes (LM2E), Institut Universitaire Européen de la Mer (IUEM), Technopole Brest-Iroise, Plouzané, France. [5]Department of Biology –Nematology research group, Ghent University campus Ledeganck K.L., Ledeganckstraat, 35 9000 Ghent, Belgium. [6]National Research Council, Institute of Ecosystem Study, Largo Tonolli 50, 28922 Verbania Pallanza, Italy. [7]Muséum National d'Histoire Naturelle Sorbonne Universités, Institut de Systématique Evolution Biodiversité, (ISYEB – UMR 7205 – CNRS, MNHN, UPMC, EPHE), 75005 Paris, France. [8]Natural History Museum of Denmark, University of Copenhagen, Øster Voldgade 5-7, 1350, Copenhagen K, Denmark. [9]Department of Biology, Marine Biology research group, Ghent University, Krijgslaan 281, S8, 9000, Ghent, Belgium.

Received: 25 July 2018 Accepted: 25 June 2019
Published online: 26 July 2019

References
1. Fouquet Y, Von Stackelberg U, Charlou JL, Donval JP, Erzinger J, Foucher JP, et al. Hydrothermal activity and metallogenesis in the Lau Basin. Nature. 1991;349:778–81.
2. Sarradin PM, Caprais JC, Riso R, Kerouel R. Chemical environment of the hydrothermal mussel communities in the lucky strike and Menez Gwen vent fields, mid Atlantic ridge. Cah Biol Mar. 1999;40:93–104.
3. Charmasson S, Sarradin PM, Le Faouder A, Agarande M, Loyen JD. High levels of natural radioactivity in biota from deep-sea hydrothermal vents: a preliminary communication. J Environ Radioact. 2009;100:522–6.
4. Cuvelier D, Beesau J, Ivanenko VN, Zeppilli D, Sarradin PM, Sarrazinet J. First insights into macro-and meiofaunal colonisation patterns on paired wood/slate substrata at Atlantic deep-sea hydrothermal vents. Deep Sea Res Part I. 2014;87:70–81.
5. Jannasch HW. Microbial interactions with hydrothermal fluids. Geophys Monogr. 1995;91:273–96.
6. Léveillé RJ, Levesque C, Juniper SK. Biotic interactions and feedback processes in deep-sea hydrothermal vent ecosystems. In: Haese RR, Kristensen K, Kostka J, editors. Interactions between macro- and microorganisms in marine sediments. Washington DC: American Geophysical Union; 2013. p. 299–321.
7. Dubilier N, Bergin C, Lott C. Symbiotic diversity in marine animals: the art of harnessing chemosynthesis. Nat Rev Microbiol. 2008;6:725–40.
8. Jeng MS, Ng NK, Ng PKL. Feeding behaviour: hydrothermal vent crabs feast on sea "snow". Nature. 2004;432:969.
9. Sarrazin J, Legendre P, deBusserolles F, Fabri MC, Guilini K, Ivanenko VN, et al. Biodiversity patterns, environmental drivers and indicator species on a high-temperature hydrothermal edifice, mid-Atlantic ridge. Deep Sea Res Part II. 2015;121:177–92.
10. Zeppilli D, Vanreusel A, Pradillon F, Fuchs S, Mandon P, James T, et al. Rapid colonisation by nematodes on organic and inorganic substrata deployed at the deep-sea lucky strike hydrothermal vent field (mid-Atlantic ridge). Mar Biodivers. 2015;45:489–504.
11. Zeppilli D, Leduc D, Fontanier C, Fontaneto D, Fuchs S, Gooday AJ, et al. Characteristics of meiofauna in extreme marine ecosystems: a review. Mar Biodivers. 2018;48:35–71.
12. Zekely J, Gollner S, Van Dover CL, Govenar B, Le Bris N, Nemeschkal H, et al. Nematode communities associated with tubeworm and mussel aggregations on the East Pacific rise. Cah Biol Mar. 2006;47:477–82.
13. Vanreusel A, Van den Bossche I, Thiermann F. Freeliving marine nematodes from hydrothermal sediments: similarities with communities from diverse reduced habitats. Mar Ecol Prog Ser. 1997;157:207–19.
14. Flint HC, Copley JTP, Ferrero TJ, Van Dover CL. Patterns of nematode diversity at hydrothermal vents on the East Pacific rise. Cah Biol Mar. 2006;47:365–70.
15. Gollner S, Zekely J, Govenar B, Le Bris N, Nemeschkal HL, Fisher CR, et al. Tubeworm-associated permanent meiobenthic communities from two chemically different hydrothermal vent sites on the East Pacific rise. Mar Ecol Prog Ser. 2007;337:39–49.
16. Gollner S, Riemer B, Martínez Arbizu P, Le Bris N, Bright M. Diversity of meiofauna from the 9°50′N East Pacific rise across a gradient of hydrothermal fluid emissions. PLoS One. 2010;5:e12321.
17. Tchesunov A. Free-living nematode species (Nematoda) dwelling in hydrothermal sites of the north mid-Atlantic ridge. Helgol Mar Res. 2015;69:343–84.
18. Smol N, Muthumbi A, Sharma J, Enoplida O. In: Schmidt-Rhaesa A, editor. H handbook of zoology Gastrotricha, Cycloneuralia, Gnathifera, vol. 2. Berlin: de Gruyter; 2014. p. 193–249.
19. Zeppilli D, Danovaro R. Meiofaunal diversity and assemblage structure in a shallow-water hydrothermal vent in the Pacific Ocean. Aquat Biol. 2009;5:75–84.
20. Thiermann F, Vismann B, Giere O. Sulphide tolerance of the marine nematode *Oncholaimus campylocercoides* a result of internal Sulphur formation? Mar Ecol Prog Ser. 2000;193:251–9.

21. Zeppilli D, Bongiorni L, Santos RS, Vanreusel A. Changes in nematode communities in different physiographic sites of the condor seamount (north-East Atlantic Ocean) and adjacent sediments. PLoS One. 2014;9: e115601.
22. Portail M, Brandily C, Cathalot C, Colaço A, Gélinas Y, Husson B, Sarradin PM, Sarrazin J. Food-web complexity across hydrothermal vents on the Azores triple junction. Deep Sea Res Part I. 2018;131:101–20.
23. Bellec L, Cambon Bonavita MA, Cueff-Gauchard V, Durand L, Gayet N, Zeppilli D. A nematode of the mid-Atlantic ridge hydrothermal vents harbors a possible symbiotic relationship. Front Microbiol. 2018;9:2246.
24. Leduc D. Description of *Oncholaimus moanae* sp. nov. (Nematoda: Oncholaimidae), with notes on feeding ecology based on isotopic and fatty acid composition. J Mar Biol Assoc UK. 2009;89:337–44.
25. Pond DW, Allen CE, Bell MV, Van Dover CL, Fallick AE, Dixon DR, Sargent JR. Origins of long-chain polyunsaturated fatty acids in the hydrothermal vent worms *Ridgea piscesae* and *Protis hydrothermica*. Mar Ecol Prog Ser. 2002; 225:219–22.
26. Wakeham SG, Hedges JI, Lee C, Peterson ML, Hernes PJ. Compositions and transport of lipid biomarkers through the water column and surficial sediments of the equatorial Pacific Ocean. Deep Sea Res Part II. 1997;44:2131–62.
27. Bolla R. Nematode energy metabolism. In: Zuckermann BM, editor. Nematodes as Biological Models. New York: Academic Press; 1980. p. 165–92.
28. Rothstein M, Götz P. Biosynthesis of fatty acids in the free-living nematode, *Turbatrix aceti*. Arch Biochem Biophys. 1968;126:131–40.
29. Boschen RE, Rowden AA, Clark MR, Gardner JPA. Mining of deep-sea seafloor massive sulfides: a review of the deposits, their benthic communities, impacts from mining, regulatory frameworks and management strategies. Ocean Coast Manag. 2013;84:54–67.
30. Ondréas H, Cannat M, Fouquet Y, Normand A, Sarradin PM, et al. Recent volcanic events and the distribution of hydrothermal venting at the lucky strike hydrothermal field, mid-Atlantic ridge. Geochem Geophys Geosyst. 2009;10:1–18.
31. Cuvelier D, Sarradin PM, Sarrazin J, Colaço A, Copley JT, Desbruyeres D, et al. Hydrothermal faunal assemblages and habitat characterisation at the Eiffel tower edifice (lucky strike, mid-Atlantic ridge). Mar Ecol. 2011;32:243–55.
32. Seinhorst JW. A rapid method for the transfer of nematodes from fixative to unhydrous glycerine. Nematologica. 1959;4:67–9.
33. Vincx M. Meiofauna in marine and freshwater sediments. In: Hall GS, editor. Methods for the examination of organismal diversity in soils and sediments. Wallingford: CAB International; 1966. p. 187–95.
34. Fontaneto D, Flot JF, Tang CQ. Guidelines for DNA taxonomy, with a focus on the meiofauna. Mar Biodivers. 2015;45:433–51.
35. Zhang J, Kapli P, Pavlidis P, Stamatakis A. A general species delimitation method with applications to phylogenetic placements. Bioinformatics. 2013; 29:2869–76.
36. Katoh K, Misawa K, Kuma KI, Miyata T. MAFFT: a novel method for rapid multiple sequence alignment based on fast Fourier transform. Nucleic Acids Res. 2002;30:3059–66.
37. Stamatakis A. RAxML version 8: a tool for phylogenetic analysis and post-analysis of large phylogenies. Bioinformatics. 2014;30:1312–3.
38. Andrassy I. The determination of volume and weight of nematodes. Acta Zool Hung. 1956;2:115.
39. Feller RJ, Warwick RM. Introduction to the study of meiofauna. In: Higgins RP, Thiel H, editors. Energetics. Washington: Smithsonian Institute Press; 1988. p. 181–96.
40. R Core Team R. A language and environment for statistical computing. Vienna www.r-project.org/: R Foundation for Statistical Computing; 2014.
41. Crepeau V, Cambon Bonavita MA, Lesongeur F, Randrianalivelo H, Sarradin PM, Sarrazin J, et al. Diversity and function in microbial mats from the lucky strike hydrothermal vent field. FEMS Microbiol Ecol. 2011;76:524–40.
42. Gebruk AV, Southward EC, Kennedy H, Southward AJ. Food sources, behaviour, and distribution of hydrothermal vent shrimps at the mid-Atlantic ridge. J Mar Biol Assoc UK. 2000;80:485–99.
43. Khripounoff A, Vangriesheim A, Crassous P, Segonzac M, Colaco A, Desbruyères D, Barthelemy R. Particle flux in the rainbow hydrothermal vent field (mid-Atlantic ridge): dynamics, mineral and biological composition. J Mar Res. 2001;59:633–56.
44. Charlou JL, Donval JP, Douville E, Jean-Baptiste P, Radford-Knoery J, Fouquet Y, et al. Compared geochemical signatures and the evolution of Menez Gwen (37°50′N) and lucky strike (37°17′N) hydrothermal fluids, south of the Azores triple junction on the mid-Atlantic ridge. Chem Geol. 2000;171:49–75.
45. Hügler M, Sievert SM. Beyond the Calvin cycle: autotrophic carbon fixation in the ocean. Ann Rev Mar Sci. 2011;3:261–89.
46. Sievert SM, Hügler M, Taylor CD, Wirsen CO. Sulfur oxidation at deep-sea hydrothermal vents. In: Dahl C, Friedrich CG, editors. Microbial Sulfur Metabolism. Berlin Heidelberg: Springer; 2008. p. 238–58.
47. Trask JL, Van Dover CL. Site-specific and ontogenetic variations in nutrition of mussels (*Bathymodiolus sp.*) from the lucky strike hydrothermal vent field, mid-Atlantic ridge. Limnol Oceanogr. 1999;44:334–43.

Publisher's Note